

Pressure-induced positive electrical resistivity coefficient in Ni-Nb-Zr-H glassy alloy

著者	Fukuhara M., Gangli C., Matsubayashi K., Uwatoko Y.
journal or publication title	Applied physics letters
volume	100
number	25
year	2012-06-18
URL	http://hdl.handle.net/10097/57352

doi: 10.1063/1.4729574

Pressure-induced positive electrical resistivity coefficient in Ni-Nb-Zr-H glassy alloy

M. Fukuhara, C. Gangli, K. Matsubayashi, and Y. Uwatoko

Citation: [Applied Physics Letters](#) **100**, 253114 (2012); doi: 10.1063/1.4729574

View online: <http://dx.doi.org/10.1063/1.4729574>

View Table of Contents: <http://scitation.aip.org/content/aip/journal/apl/100/25?ver=pdfcov>

Published by the [AIP Publishing](#)

Articles you may be interested in

[Proton nuclear magnetic resonance studies of hydrogen diffusion and electron tunneling in Ni-Nb-Zr-H glassy alloys](#)

J. Appl. Phys. **111**, 124308 (2012); 10.1063/1.4729544

[Electronic transport behaviors of Ni-Nb-Zr-H glassy alloys](#)

J. Appl. Phys. **107**, 033703 (2010); 10.1063/1.3284207

[ac impedance analysis of a Ni-Nb-Zr-H glassy alloy with femtofarad capacitance tunnels](#)

Appl. Phys. Lett. **96**, 043103 (2010); 10.1063/1.3294294

[Local atomic structure around Ni, Nb, and Zr atoms in Ni-Nb-Zr-H glassy alloys studied by x-ray absorption fine structure method](#)

J. Appl. Phys. **105**, 113527 (2009); 10.1063/1.3143039

[Coulomb oscillation of a proton in a Ni-Nb-Zr-H glassy alloy with multiple junctions](#)

Appl. Phys. Lett. **90**, 203111 (2007); 10.1063/1.2739080



AIP | Journal of
Applied Physics

Journal of Applied Physics is pleased to
announce **André Anders** as its new Editor-in-Chief

Pressure-induced positive electrical resistivity coefficient in Ni-Nb-Zr-H glassy alloy

M. Fukuhara,^{1,2} C. Gangli,³ K. Matsubayashi,³ and Y. Uwatoko³

¹Institute for Materials Research, Tohoku University, Sendai 980-8577, Japan

²Research Institute for Electromagnetic Materials, Sendai, 982-0807, Japan

³Institute for Solid State Physics, University of Tokyo, Chiba 277-8581, Japan

(Received 13 March 2012; accepted 1 June 2012; published online 21 June 2012)

Measurements under hydrostatic pressure of the electrical resistivity of $(\text{Ni}_{0.36}\text{Nb}_{0.24}\text{Zr}_{0.40})_{100-x}\text{H}_x$ ($x = 9.8, 11.5,$ and 14) glassy alloys have been made in the range of 0–8 GPa and 0.5–300 K. The resistivity of the $(\text{Ni}_{0.36}\text{Nb}_{0.24}\text{Zr}_{0.40})_{86}\text{H}_{14}$ alloy changed its sign from negative to positive under application of 2–8 GPa in the temperature range of 300–22 K, coming from electron-phonon interaction in the cluster structure under pressure, accompanied by deformation of the clusters. In temperature region below 22 K, the resistivity showed negative thermal coefficient resistance by Debye-Waller factor contribution, and superconductivity was observed at 1.5 K. © 2012 American Institute of Physics. [<http://dx.doi.org/10.1063/1.4729574>]

With recent advances in hydrogen permeability as an energy source using melt-spun flexible amorphous Ni-Nb-Zr-H glassy alloys,¹ attention is also being paid to their electronic applications. Recently, we reported the electronic transport behavior of $(\text{Ni}_{0.6}\text{Nb}_{0.4})_{1-x}\text{Zr}_x)_{100-y}\text{H}_y$ ($0.3 \leq x \leq 0.5, 0 \leq y \leq 20$) glassy alloys as a function of their hydrogen content.² These alloys showed semiconducting-like behavior, superior (ballistic) conducting and superconducting transport, and electric current-induced voltage (Coulomb) oscillation as the hydrogen content increased. The alloy can be regarded as a dc/ac converting device with a large number of 0.23-nm-sized capacitors with femtofarad capacitance³ among the electron-conducting distorted icosahedral $\text{Zr}_5\text{Ni}_5\text{Nb}_3$ clusters (dots of ~ 0.55 nm in size⁴). When a hydrogen atom localizes at the two stable and four metastable H sites in the cluster during electrolysis, it is dissociated into a proton and electron, and the liberated electron forms a localized state coupled with Zr and Nb atoms.^{4,5} Furthermore, we assumed that the superconductivity of these glassy alloys is associated with electron pair transport along zigzag paths, which link the shortened atomic -Ni-Ni-Ni- array in the $\text{Zr}_5\text{Ni}_5\text{Nb}_3$ clusters and tunnel among them.⁶ From these electronic behaviors,²⁻⁶ we infer that the $\text{Zr}_5\text{Ni}_5\text{Nb}_3$ cluster coupled with H plays a decisive role in the promising electronic properties observed in these amorphous alloys, as well as in the familiar Perovskite crystal phase.

It is also important to examine the pressure dependence of electron transport behavior in order to fully understand cluster morphology in glassy alloys. Our interests lie in investigating pressure effects on the resistance properties of $(\text{Ni}_{0.36}\text{Nb}_{0.24}\text{Zr}_{0.40})_{100-x}\text{H}_x$ ($x = 9.8, 11.5,$ and 14) glassy alloys in terms of their cluster configuration. No previous paper has reported this for glassy alloys with hydrogen.

The electrical resistance of glassy alloys has been measured by many groups.⁷⁻⁹ Mooij¹⁰ showed empirically the presence of a strong correlation between thermal coefficient resistance (TCR) and electrical resistivity ($\rho_{300\text{K}}$) at room temperature for many transition metal alloys; the TCR changes its sign from positive to negative when $\rho_{300\text{K}}$ exceeds about $150 \mu\Omega\text{cm}$, regardless of whether the alloy is

in a crystalline state or an amorphous one. Mizutani¹¹ classified their resistances in view of the magnetic state, on which the electronic state and electron transport property heavily depend; (1) ferromagnetism, (2) weak ferromagnetism, (3) spin glass and Kondo states, (4) paramagnetism, and (5) very weak paramagnetism or diamagnetism. The glassy alloy used in this study belongs to group (4), and its resistivity at 300 K is higher than $150 \mu\Omega\text{cm}$ before charging hydrogen and loading pressure.

Amorphous $\text{Ni}_{36}\text{Nb}_{24}\text{Zr}_{40}$ alloy ribbons of about 1-mm width and 30- μm thickness were synthesized from argon arc-melted ingots using free-jet melt spinning in Ar at a rotation speed of 3000 rpm (31.6 m/s). Hydrogen charging was carried out electrolytically in 0.5 M H_2SO_4 and 1.4 g/L thiourea (H_2NCSNH_2) at room temperature with current densities of 30 A/m^2 , using a Pt counter electrode. To guarantee homogeneous distribution of hydrogen, we used the specimens one week after their charging. The specimens were adjusted to the same resistivity before and after polishing on both sides by $5 \mu\text{m}$.¹² The details of the procedure have been described in previous papers.²⁻⁶

Electrical resistivity was measured under applied high pressure of up to 8 GPa from 300 down to 2 K using a standard dc four-probe method.¹³ Hydrostatic pressure was generated by a cubic anvil cell (CAC) with a 250 ton press. We used a 1:1 mixture of fluorinates FC70 and FC77 as a pressure-transmitting medium. The sample specimens had dimensions of $0.8 \times 0.4 \times 0.03$ mm. Electrical contacts to the specimen were made with 20 μm diameter gold wires and conducting silver paste. In order to determine precisely the resistivity at 300 K, we calculated it using compressibility of 0.00758/GPa. Since the maximum deviation in length under hydrostatic pressure of 8 GPa is 1.8%, we did not correct the observed data in this study.

For calculation of the Debye temperature D_θ ,¹⁴ based on ultrasonic method, we used 3 degrees of freedom and $5.06 \times 10^{-29} \text{ m}^3$ as an average atomic volume. D_θ is calculated as 278.9 K, using $V_l = 5298 \text{ m/s}$ and $V_s = 2121.5 \text{ m/s}$,¹⁵ where V_l and V_s are longitudinal and transverse wave velocity, respectively.

The electrical resistances of the $(\text{Ni}_{0.36}\text{Nb}_{0.24}\text{Zr}_{0.40})_{90.2}\text{H}_{9.8}$ and $(\text{Ni}_{0.36}\text{Nb}_{0.24}\text{Zr}_{0.40})_{98.5}\text{H}_{11.5}$ glassy alloys were measured at 0.1 MPa during cooling and heating runs. The results are shown as a function of temperature T in Fig. 1. The resistivity of $(\text{Ni}_{0.36}\text{Nb}_{0.24}\text{Zr}_{0.40})_{90.2}\text{H}_{9.8}$ increased almost linearly with a negative TCR of $-1.77 \times 10^{-4}/\text{K}$ down to 2.2 K, except for one peak at 12 K and one valley at 7 K, and then abruptly dropped from 2 K. The sample showed zero resistivity at 1.9 K (inset in Fig. 1). It is well known that a negative TCR, which has also been observed in $(\text{Ni}_{0.36}\text{Nb}_{0.24}\text{Zr}_{0.40})_{90.1}\text{H}_{9.9}$ glassy alloy under ambient pressure,² occurs through weak localization effects in a metallic regime, where the density of states at the Fermi level must be finite. During the heating run, the resistivity decreased following the same curve as the cooling run, except for a variation between 20 and 42 K. This variation is attributed to a current-induced voltage oscillation, known as Coulomb oscillation under ambient pressure.² The reason why this temperature dependence is only the heating run has been already explained by different degree of amorphousness between cooling and heating runs.¹⁶ The low-temperature drops noted in the two runs mirror the normal-to-superconducting transitions. In a previous paper,¹⁷ $(\text{Ni}_{0.36}\text{Nb}_{0.24}\text{Zr}_{0.40})_{94.4}\text{H}_{5.4}$ glassy alloy showed type II superconductivity at 2.1 K under ambient pressure. On the other hand, the whole resistivity of the $(\text{Ni}_{0.36}\text{Nb}_{0.24}\text{Zr}_{0.40})_{98.5}\text{H}_{11.5}$ glassy alloy showed similar behaviors to $(\text{Ni}_{0.36}\text{Nb}_{0.24}\text{Zr}_{0.40})_{90.2}\text{H}_{9.8}$ alloy under ambient pressure. However, the $(\text{Ni}_{0.36}\text{Nb}_{0.24}\text{Zr}_{0.40})_{98.5}\text{H}_{11.5}$ alloy did not show Coulomb oscillation under pressure. It has already been reported that this oscillation occurs in a restricted region of 30–45 at. % Zr and 5–12 at. % H under ambient pressure.^{2,16} The onset superconducting temperature (T_o) and superconducting temperature (T_c) of the $(\text{Ni}_{0.36}\text{Nb}_{0.24}\text{Zr}_{0.40})_{98.5}\text{H}_{11.5}$ alloy are 2.2 and 2.1 K, respectively (see inset of Fig. 1). Consequently, resistivity behaviors under 0.1 MPa are almost the same without application of pressure.

To confirm the pressure dependence of resistivity, we measured the resistivity under 0.1 MPa, and at 2, 5, and 8 GPa, using a $(\text{Ni}_{0.36}\text{Nb}_{0.24}\text{Zr}_{0.40})_{86}\text{H}_{14}$ glassy alloy, which does not show Coulomb oscillation. Fig. 2 shows the pressure effect on temperature dependent resistivity during the

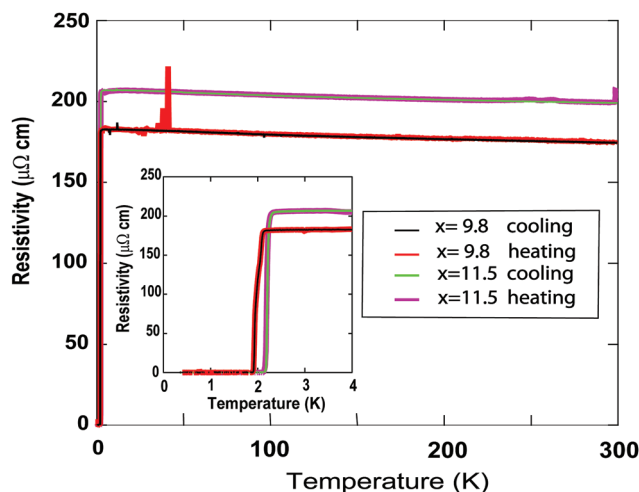


FIG. 1. Electric resistivities of the $(\text{Ni}_{0.36}\text{Nb}_{0.24}\text{Zr}_{0.40})_{90.2}\text{H}_{9.8}$ and $(\text{Ni}_{0.36}\text{Nb}_{0.24}\text{Zr}_{0.40})_{88.5}\text{H}_{11.5}$ glassy alloys under 0.1 MPa during cooling and heating runs. Inset: Details of resistivity at around T_c .

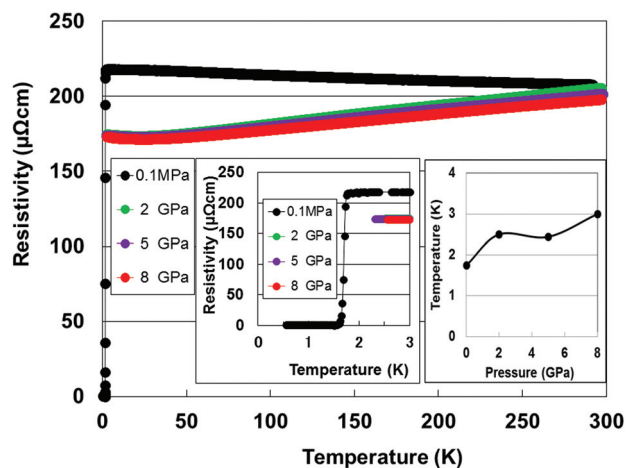


FIG. 2. Temperature dependence of the resistivity of $(\text{Ni}_{0.36}\text{Nb}_{0.24}\text{Zr}_{0.40})_{86}\text{H}_{14}$ under hydrostatic pressure. Inset: Details of resistivity at 2, 5, and 8 GPa and pressure dependence of T_o .

heating run. The resistivity under 0.1 GPa pressure showed similar behavior ($T_c = 1.6$ K, inset in Fig. 2) to the $(\text{Ni}_{0.36}\text{Nb}_{0.24}\text{Zr}_{0.40})_{98.5}\text{H}_{11.5}$ alloy. However, the resistivity under 2, 5, and 8 GPa decreased with positive TCR as the temperature decreased and the pressure increased. This result is an evidence of a pressure-induced electronic conducting transition. Although glassy alloys with $\rho_{300\text{K}}$ below $150 \mu\Omega\text{cm}$ generally show positive TCR,¹¹ subject to the electron-phonon interaction, there are no previous reports of positive TCR for alloys with $\rho_{300\text{K}}$ over $200 \mu\Omega\text{cm}$. This is in conflict with the Mooij relation and thus is taken as a very unusual finding. Positive TCR is also often observed in metallic crystals. The alloy showed superconductivity at 1.5 K, but we could not observe resistivity below 2.5 K under 2, 5, and 8 GPa because of the sample breaking. However, the pressure dependence of T_o inset in Fig. 2 shows an increase in T_o with increasing pressure.

Enlarging resistivity curves of the temperature region below 100 K measured under 2, 5, and 8 GPa, a resistivity minimum is clearly observable at 22–25 K (Fig. 3). Minimum values of resistivity and the corresponding temperature are shown in inset in Fig. 3 as a function of pressure P . The

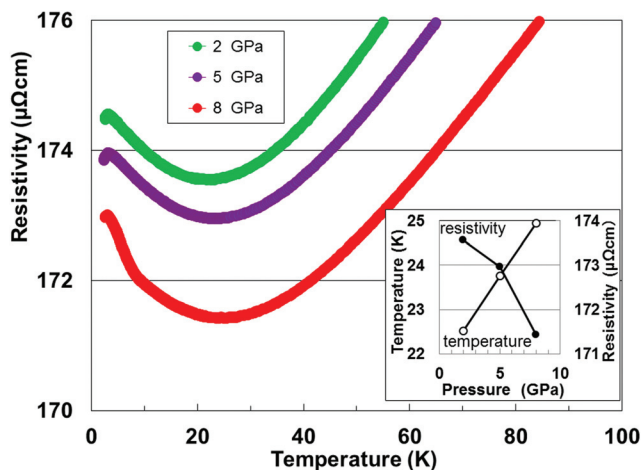


FIG. 3. Enlarged resistivity curves of the temperature region below 100 K under 2, 5, and 8 GPa. Inset: Pressure dependence of minimum values of resistivity and corresponding temperature.

minimum resistivity and the corresponding temperature linearly decrease and increase with increasing pressure, respectively. The resistivity with negative TCR in the temperature region below 22 K is attributed to an intrinsic amorphous character of metal-metal type glassy alloys, suggesting the survival of the cluster structures. As the present electrical resistivity model for glassy alloys, we know an extended Ziman theory, based on the Boltzmann transport equation;¹⁷ the temperature dependence of the resistivity is given by

$$\rho(T) = \exp(-2W(T))(\rho_0 + \Delta\rho), \quad (1)$$

where $\exp(-2W(T))$, ρ_0 , and $\Delta\rho$ are the Debye-Waller factor, residual resistivity, and electron-phonon interaction, respectively. However, since extended Ziman theory cannot be applied to transition metals, where the scattering due to transition metal elements is too strong to validate the second-order perturbation theory, the application of the theory is inappropriate in the present samples.

Apart from the extended Ziman theory, Debye-Waller factor contributes to a negative T^2 dependence at low temperatures and a negative T dependence at high temperatures. Since the electron-phonon interaction provides increases in resistivity with increasing temperature, taking into consideration nonelastic scattering of electrons by lattice vibration, the resistivity with positive TCR in the temperature region above 22 K under pressures of 3, 5, and 8 GPa could be derived from electron-phonon interaction in the cluster structure under pressure, accompanied by deformation of clusters. This would be caused by enhancement in metallic like rigidity, associated with a relative increase of covalency by metal hydrogenation under high compression. The resistivity minimum at 22–25 K is an equilibrium temperature for both antinomic effects.

The origin for the resistivity minimum is explained by two mechanisms, the Kondo effect¹⁸ and a structural effect.¹¹ Here, we note that Cochrane *et al.*¹⁹ asserted that the resistivity minimum arises from the disordered arrangement of atoms in glassy alloys and is entirely nonmagnetic in origin. In their model, some sites exist in glassy alloys in which the atoms are in double-potential wells, providing the possibility of electron scattering from tunneling levels, although most experiments had been carried out on magnetically impure materials. Since the glassy alloy used in this study contains ferromagnetic Ni, the origin would be due to

either the structural effect or the Kondo effect. However, we have no data for the Kondo effect. Furthermore, Fritsch *et al.*²⁰ have reported pressure dependences of resistivity for $\text{Mg}_{70}\text{Zn}_{30}$, $\text{Cu}_{57}\text{Zr}_{43}$, and $\text{Ti}_{50}\text{Be}_{40}\text{Zr}_{10}$; their TCRs maintained negative values and did not change sign from negative to positive.

On the other hand, the three curves revealed maximum values at 2–3 K, suggesting an onset-temperature of superconductivity at this temperature. Because T_o increases with increasing pressure (Fig. 2, inset), application of pressure induces shrinkage of the atomic distances at the neighbor Ni sites in the $\text{Zr}_5\text{Ni}_5\text{Nb}_3$ cluster.⁶ Increase in T_o has been associated with increase in shrinkage.²¹

Further study is needed for mechanism of pressure-induced resistivity. We must also address hydrogen dependence of resistivity at 300 K and T_o .

¹S. Yamaura, M. Sakurai, M. Hasegawa, K. Wakoh, Y. Shimpo, M. Nishida, H. M. Kimura, E. Matsubara, and A. Inoue, *Acta Mater.* **53**, 3703 (2005).

²M. Fukuhara, H. Yoshida, K. Koyama, A. Inoue, and Y. Miura, *J. Appl. Phys.* **107**, 033703 (2010).

³M. Fukuhara, M. Seto, and A. Inoue, *Appl. Phys. Lett.* **96**, 043103 (2010).

⁴M. Fukuhara, N. Fujima, H. Oji, A. Inoue, and S. Emura, *J. Alloy Compd.* **497**, 182 (2010).

⁵H. Oji, K. Handa, J. Ide, T. Honda, S. Yamaura, A. Inoue, N. Umesaki, S. Emura, and M. Fukuhara, *J. Appl. Phys.* **105**, 113527 (2007).

⁶M. Fukuhara, H. Yoshida, K. Koyama, A. Inoue, and Y. Miura, *J. Nanosci. Nanotech.* **10**, 4975 (2010).

⁷S. M. Girvin and M. Jonson, *Phys. Rev. B* **22**, 3583 (1980).

⁸T. A. Stephens, D. Rathnayaka, and D. G. Naugle, *Mater. Sci. Eng. A* **133**, 59 (1991).

⁹O. Haruyama, H. Kimura, A. Inoue, and N. Nishiyama, *Appl. Phys. Lett.* **76**, 2026 (2000).

¹⁰J. H. Mooij, *Phys. Status Solidi A* **17**, 521 (1973).

¹¹U. Mizutani, *Prog. Mater. Sci.* **28**, 97 (1983).

¹²M. Fukuhara and Y. Umemori, *Int. J. Mol. Sci.* **13**, 180 (2012).

¹³N. Mori, H. Takahashi, and Takeshita, *High Press. Res.* **24**, 225 (2004).

¹⁴O. L. Anderson, *J. Phys. Chem. Solids* **12**, 41 (1959).

¹⁵M. Fukuhara and H. Yoshida, *J. Non-Cryst. Sol.* **358**, 959 (2012).

¹⁶M. Fukuhara, "Rotating speed effect on electronic transport behaviors of Ni-Nb-Zr-H glassy alloys," *J. Alloy Compd.* (in press).

¹⁷J. M. Ziman, *Principles of the Theory of Solids*, 2nd ed. (Cambridge University Press, London, 1972).

¹⁸J. Kondo, *Prog. Theor. Phys.* **32**, 37 (1964).

¹⁹R. W. Cochrane, R. Harris, J. O. Ström-Olsen, and M. J. Zuckermann, *Phys. Rev. Lett.* **35**, 676 (1978).

²⁰G. F. Fritsch, J. Willer, A. Wildermuth, and E. Lüscher, *J. Phys. F: Met. Phys.* **12**, 2965 (1982).

²¹F. Fukuhara, *Phys. Status Solidi B* **175**, 421 (1993).